Physical Science International Journal

Volume 26, Issue 7, Page 1-10, 2022; Article no.PSIJ.93762
ISSN: 2348-0130

Computational Nanomaterials Design: Towards the Realization of Nanoparticle use in Radiotherapy Case Study 2: Adsorption states of At on Au (111) Surface

Jeffrey Tanudji [a], Susan Meñez Aspera [b], Hideaki Kasai [a,b,c*], Michio Okada [c,d], Tetsuo Ogawa [c,e] and Hiroshi Nakanishi [b]

[a] Department of Applied Physics, Graduate School of Engineering, Osaka University, 1-1 Yamadaoka, Suita, Osaka-565-0871, Japan.
[b] National Institute of Technology, Akashi College, 679-3 Nishioka, Uozumi-cho, Akashi, Hyogo-674-8501, Japan.
[c] Institute of Radiation Sciences, Osaka University, 1-1 Machikaneyama-cho, Toyonaka, Osaka-560-0043, Japan.
[d] Department of Chemistry, Graduate School of Science, Osaka University, 1-1 Machikaneyama-cho, Toyonaka, Osaka-560-0043, Japan.
[e] Department of Physics, Graduate School of Science, Osaka University, 1-1 Machikaneyama-cho, Toyonaka, Osaka-560-0043, Japan.

Authors' contributions

This work was carried out in collaboration among all authors. All authors read and approved the final manuscript.

Article Information

DOI: 10.9734/PSIJ/2022/v26i7752

Open Peer Review History:
This journal follows the Advanced Open Peer Review policy. Identity of the Reviewers, Editor(s) and additional Reviewers, peer review comments, different versions of the manuscript, comments of the editors, etc are available here: https://www.sdiarticle5.com/review-history/93762

Original Research Article

Received: 17/09/2022
Accepted: 19/11/2022
Published: 26/11/2022

**Corresponding author: E-mail: kasai@dyn.ap.eng.osaka-u.ac.jp;*

ABSTRACT

Astatine-211 (^{211}At or simply At) used as an α particle emitter is currently gaining as treatment method for cancer cells. It must however be attached to a carrier to facilitate the treatment process. Gold nanoparticle is a good candidate that has been used in several tests. Knowing the physics behind the adsorption of astatine on gold nanoparticles would be advantageous in designing a more optimal method for such applications. We therefore performed density functional theory calculation on astatine adsorption on gold (111) surface to understand both the mechanism of astatine bonding with gold and the strength of the bonding. We found the mechanism of adsorption to be the hybridization between the 6p orbital of astatine and the 5d and 6s orbitals of the gold. We also found the adsorption strength of astatine on gold to be -1.43 eV at the fcc hollow site. Both results provide us with a good starting point towards our goal of designing an optimized gold nanoparticle for radiotherapy.

Keywords: Computational materials design; radionuclide adsorption strength; adsorption on gold surface.

1. INTRODUCTION

Cancer is considered as one of the most deadly diseases in this world. Over 9 million people have died from cancer in the year 2020 alone [1]. Therefore, many researches are being done to treat this disease. One way in which cancer cells can be treated is by targeted α radiotherapy. Simply put, α particle emitters (isotopes that release α particles as they undergo radioactive decay) are inserted via some medium into the vicinity of the cancer cells. This allows for a localized treatment on the cancer cells.

To take advantage of this new treatment, the use of astatine in radiotherapy research has been gaining in recent years. Astatine has a shorter half-life than other α particle emitters which makes it less likely to stay active for long periods of time in the patient's body, but not so short that it is not logistically viable to be used [2-9].

To ensure the treatment goes to the right targets, it needs to be trackable inside the body. The mechanism of labeling allows for this purpose, whereby an object (e.g. protein) is labeled (or implanted) with a radioactive substance on its surface to enable external tracking for the said object when inserted into the test subject. In the work of Kato et al., the astatine is labeled onto gold nanoparticles of different sizes before being injected into the test subjects as α radiotherapy treatment [2]. The result is promising, as it shows the cancer cells growing much slower in the presence of the α particle treatment. Importantly, it also shows that the gold nanoparticles are able to hold onto the astatine for the duration of the testing. This presents great potential for future utilization since detached astatine particles can accumulate in other organs of the body such as the thyroid, stomach, etc. where they could cause unintended side effects [10].

Gold and, by extension, gold nanoparticles (AuNPs) have been used in applications such as electronics, catalysis, and biomedicine due to the many advantageous properties that they possess [11-18]. Synthesis of AuNPs can be tailored depending on the desired uses, and AuNPs are also deemed to be suitable for biomedical applications due to their low toxicity and ability to penetrate deep into cells [7,9,16-23]. Many applications for AuNPs have been developed including as drug carriers, tumor imaging, hyperthermia, etc [16-18]. AuNPs can also be used to carry out radiotherapy by being labeled with radioactive materials such as ^{225}Ac, ^{227}Th, and ^{125}I among others [10,24,25]. The additional advantage of using such methodology can be summed up in the article by Daems et al., whereby AuNPs are augmented with imaging or other treatment drugs in order to assist with the detection and/or treatment of the cancer cells [26].

Computational Materials Design (CMD®) is a design tool developed to provide a theoretical based simulation of materials where one can tool the desired properties to match the materials' end purpose [27]. By using this method we can design an optimized AuNPs as astatine carriers for radiotherapy. Some examples of works relating to CMD® are fuel cells, hydrogen fuel storage, nitric oxide (NO) catalyst, and investigation of melanin chemistry among others [28-32].

Previous works done in this field show that AuNPs are capable of carrying astatine to the

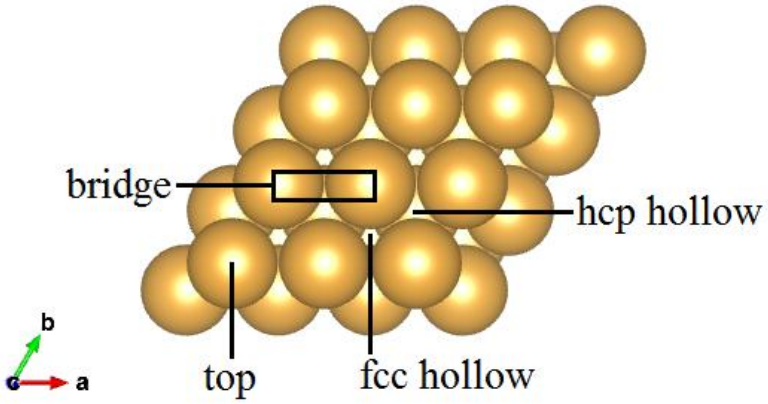

Fig. 1. Adsorption sites of Au (111) surface

cancer cells. However, relatively few have looked at the theoretical aspect of the adsorption of astatine on gold [33,34]. We would therefore like to establish the principles of adsorption of astatine on gold, before venturing into the task of finding the best AuNP structure and different astatine coverages to yield the most optimum result for this radioactive treatment.

2. METHODOLOGY

First principles calculation based on the density functional theory (DFT) were performed using the Vienna ab initio simulation package (VASP) [35,36]. The generalized gradient approximation (GGA) with Perdew, Burke, and Ernzerhof (PBE) exchange-correlation functional was used [37]. Calculations with van der Waals interaction (vdW) utilize the DFT-D3 code based on the work done by Grimme et al. [38]. The electronic one-particle wavefunctions were expanded in a plane-wave basis set up to an energy cutoff of 400 eV, while the core electrons were described by the projector augmented wave (PAW) method [39, 40]. Convergence criterion for the electronic self-consistency calculation energy is set at 10^{-5} eV and the integration for the first Brillouin zone is performed using a mesh of 5x5x1 k-points with a Monkhorst-Pack sampling scheme [41].

The calculation model is done using a 3x3 slab of 5 layers of Au(111) separated by a vacuum of 12 Å. The bottom 2 layers are kept fixed in the bulk configuration while the top three layers are allowed to relax. A schematic of the clean Au(111) surface is shown in Fig. 1 with possible adsorption sites labeled.

The preliminary calculation to optimize the gold bulk lattice constant yields a value of 4.17 Å for non-vdW case and 4.12 Å for vdW case, both of which are in good agreement with the value of 4.0786 Å, given in the CRC Handbook of Chemistry and Physics [42]. Finally, the adsorption energies for At/Au(111) can be calculated by the equation

$$E_{bonding} = E_{At/Au(111)} - \left(0.5 \times E_{At_2}\right) - E_{Au(111)} \quad (1)$$

where $E_{bonding}$ represents the adsorption energy, $E_{At/Au(111)}$ represents the energy of a single At atom adsorbed on Au(111) slab, E_{At_2} is the energy of the isolated At_2 molecule and $E_{Au(111)}$ is the energy of the clean Au(111) slab.
Additionally, Bader charge calculations are also done to obtain the charge transfers that happen during the adsorption process [43]. The Bader charge calculations involve only the valence electrons, since they are important in interatomic bonding, given by the electronic configurations of the two elements. The valence electrons being considered are $5d^{10}$ $6s^2$ $6p^5$ for At and $5d^{10}$ $6s^1$ for Au. For the purposes of analyzing the Bader charge calculations, negative values indicate an excess of electrons while positive values indicate a shortage of electrons.

3. RESULTS AND DISCUSSION

The molecular state of At_2 is considered as being theoretically stable. At does not exist stably in standard temperature and pressure (STP) conditions and as such the experimental data for At_2 has yet to be verified [42]. However, as reference for the adsorption energies, we believe this provides a good baseline since At is still a halogen and therefore would theoretically

be most stable as a molecule. The basis for modeling nanoparticle as a slab surface comes from the findings obtained by Kleis et al. [44]. The work found that as nanoparticle sizes increase above a certain threshold, the adsorption characteristics of the incoming adsorbate approaches the characteristics of that of a slab surface. This approximation allows for representation of bigger nanoparticle sizes which may contain hundreds of atoms as surface slabs and therefore removes additional burden to the computational process. It is also worth noting that for a nanoparticle, various surface facets may be present and the choice for a (111) surface is taken due to it being the most stable among the surfaces [45,46].

The results of the adsorption energy calculations of At/Au(111) are presented in table 1, with four possible adsorption sites being considered, as shown in Fig. 1.

The calculations show that the preferred site for adsorption of At is the hollow site, followed by the bridge site while the top site is less preferred for adsorption. A comparison between the calculated energies and the experiment value of -1.6 eV shows the vdW case to give a more accurate adsorption energy result compared to the non-vdW case [33]. Finally, while both hollow sites are good places for At adsorption, future calculations of At/Au (111) system will be carried out with At adsorbed on the fcc hollow site.

Table 1. Adsorption energies of at on different Au (111) sites

Position	Adsorption energy (w/o vdW) [eV]	Adsorption energy (w/ vdW) [eV]
bridge	-0.854	-1.375
fcc hollow	-0.916	-1.428
hcp hollow	-0.903	-1.424
top	-0.622	-1.204

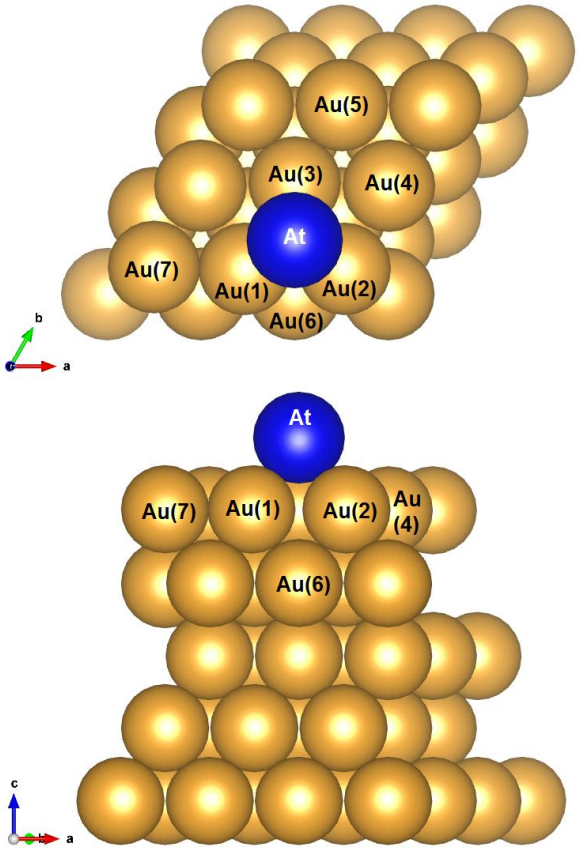

Fig. 2. Diagrams showing top view (above) and side view (below) of At adsorption on Au(111) surface

Fig. 2 shows At adsorption on Au(111) at the fcc site with labeled atoms Au(1)-Au(5) and Au(7) on the first layer (surface) and Au(6) on the second layer (first subsurface layer). The upper figure shows the system viewed from top, and the bottom figure shows the system viewed from the side. Au(1), Au(2), and Au(3) are the closest Au atoms to the adsorbing At atom, and therefore represent the atoms that will directly be affected by the approach of At. Au(4), Au(5), and Au(7) are present to show the extent of the interaction due to the adsorption of At on the fcc hollow. The distances of the final adsorption configuration is given in table 2 (refer to Fig. 2).

As explained earlier the vdW calculation yields a more accurate energy for the adsorption process. However, we decide to include the non-vdW calculation to look at the general trend of adsorption between At and Au. We see an expansion of the gold atoms surrounding the fcc hollow site (Au(1)-Au(3)) possibly due to adjustment of bond length between At-Au. Both At and Au are large atoms and therefore have large atomic radii. Interestingly, this separation between the nearby gold atoms indicate that the At-Au bonding is stronger than Au-Au bonding, which further supports the adsorption energy findings.

Overall similarities between the vdW and non-vdW calculations indicate that the trend of adsorption is the increasing “hole” size around the fcc hollow due to the nearby Au atoms moving away from the At. This causes the distances of some Au atoms to reduce and therefore become constricted in movement on the surface, again supporting the earlier finding that the At-Au bonding is stronger than Au-Au bonding.

Table 3 compares the results of the Bader charge calculation before and after At adsorption on Au (111) surface. The results indicate no significant difference in charges before and after the adsorption process, i.e. the electrons are shared between the At and the nearest Au atoms. At gains a slight positive charge while the charges in the Au slab are unaffected. It can be said therefore that the bonding between At and Au to be non-polar or covalent in nature.

Table 2. Distances between selected atoms in At/Au(111) system

Atoms	Distance (w/o vdW) [Å]	Distance (w/ vdW) [Å]
At-Au(1)		
At-Au(2)	2.962	2.952
At-Au(3)		
Au(1)-Au(2)		
Au(2)-Au(3)	3.139	3.102
Au(1)-Au(3)		
Au(3)-Au(4)	2.975	2.934
Au(4)-Au(5)	2.943	2.907
Au(1)-Au(6)	2.993	2.962
Au(2)-Au(6)		
Au(1)-Au(7)	2.854	2.819
Bulk Au	2.949	2.913

Table 3. Bader charges of At/Au(111) system

Atom	Relative charge (before adsorption) [e/atom]	Relative charge (after adsorption) [e/atom]	Difference [e/atom]
At	0	-0.0292	-0.0292
Au(1)	0.0304	0. 0282	-0.0022
Au(2)	0.0304	0. 0269	-0.0035
Au(3)	0.0304	0.0349	0.0045
Au(4)	0.0352	0. 0196	-0.0156

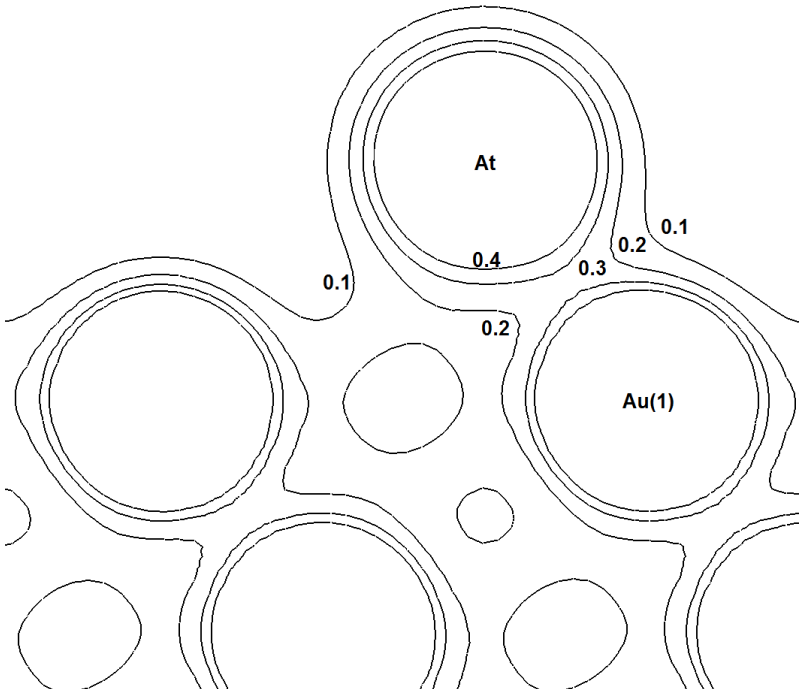

Fig. 3. Charge distribution in At/Au(111) taken at the $(\bar{1}10)$ plane

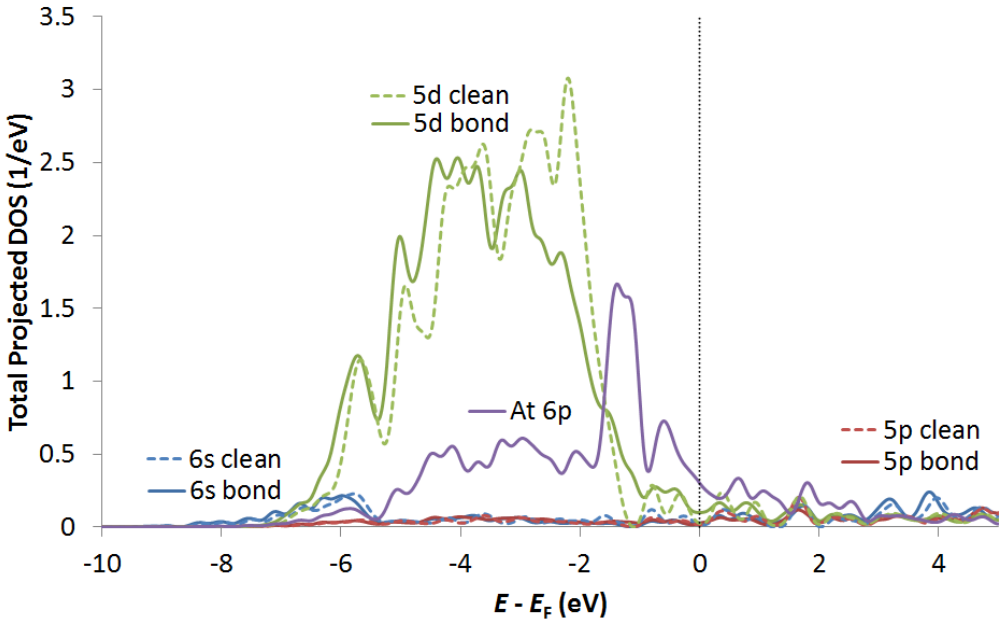

Fig. 4. DOS of At/Au(111)

The presence of bonding can be seen in Fig. 3 between the At atom (topmost atom) and the neighboring Au atom (Au) (1). The lines with values on them are contour lines expressing the delineation of charge per unit volume, with 0.1 e/Å^3 intervals between each line. Only one bonding is shown since it was found that At bonded with all three nearby Au atoms and that all the bonding strengths are similar to one another. It can be seen that there is a slightly higher electron concentration between the At and Au (1), indicating that both At and the corresponding Au atoms are sharing electrons. Considering the symmetry to the other two

nearest neighbors (Au(2) and Au(3)), the amount of electrons being shared is actually three times larger than what can be shown in this figure. To get a more in depth perspective, we shall look at the electronic states of the system.

Fig. 4 shows the density of states (DOS) of the Au(1) valence orbitals along with the At 6p orbital after adsorption. The dotted lines represent a clean Au surface (before adsorption) while the bold lines represent the Au orbitals after bonding with At (after adsorption). The purple line is the At 6p orbital after undergoing adsorption. We can see that the Au orbital changes before and after adsorption indicating the interaction between Au and At which gives rise to bonding.

Previous results have shown the bonding between At and Au to be covalent, due to the lack of charge transfer between the two elements. An indicator for this bonding is the presence of hybridization between orbitals of different reactants. In Fig. 4, we can see that the DOS of Au 5d “bond” orbital and the DOS of At 6p orbital are closely linked, indicating that both orbitals are affecting each other. Hybridization of the Au 5d and At 6p takes place around the -4.5 eV to -2 eV, giving rise to a higher presence of lower energy regions. These lower energy regions are occupied by the bonding electrons, providing a more stable adsorption profile for the At on Au. We also find a smaller hybridization taking place between the At 6p and Au 6s orbitals around -6 eV. These two hybridization profiles strengthen our finding that covalent bonding is the primary reason of the bonding between At and Au.

4. CONCLUSIONS

In this work, we have calculated the adsorption states of astatine on gold (111) surface to find the nature of the bonding between astatine and gold and also obtain a quantitative value for the strength of said bonding. The calculation results indicate that the astatine absorbs on hollow sites of the gold (111) surface with an adsorption energy of -1.43 eV. This bonding is of a covalent nature and is due to the hybridization of the astatine 6p orbital with the gold 5d orbital. Van der Waals interaction does not alter the characteristics of the bonding but offers more accurate adsorption energy as obtained by experiment. Understanding how astatine adsorbs on the gold (111) surface is a first step for us to construct a model by which we can experiment with other configurations and find out the relative strength of the bonding, as well as study the effect of radiation on the gold nanoparticles themselves. With this result, we hope to open a new field of application for CMD® to design optimized gold nanoparticles for the purposes of treating various cancer diseases.

ACKNOWLEDGEMENT

Calculations were performed in Nano-Design Lab of Nakanishi laboratory at the National Institute of Technology, Akashi College, as well as the Yukawa Institute for Theoretical Physics (YITP) Supercomputer at Kyoto University. JT gratefully acknowledges the fruitful discussions with Prof. W. A. Diño as well as the financial support provided by the Matsuda Yosahichi Memorial Foundation for Foreign Students and Osaka University.

COMPETING INTERESTS

Authors have declared that no competing interests exist.

REFERENCES

1. International Agency for Research on Cancer. All cancers. Available:https://gco.iarc.fr/today/data/factsheets/cancers/39-All-cancers-fact-sheet.pdf” Online (2020) (Retrieved 2022-10-31).
2. Kato H, Huang X, Kadonaga Y, Katayama D, Ooe K, Shimoyama A, Kabayama K, Toyoshima A., Shinohara A, Hatazawa J, and K. Fukase. Intratumoral administration of astatine-211-labeled gold nanoparticle for alpha therapy. J. Nanobiotechnol. 19, 223 (2021). Available: https://doi.org/10.1186/s12951-021-00963-9
3. Sgouros G, Roeske JC, McDevitt MR, Palm S, Allen BJ. SNM MIRD Committee: Bolch WE, Brill AB, Fisher DR, Howell RW, Meredith RF, Sgouros G, Wessels BW, Zanzonico PB: MIRD Pamphlet No. 22 (abridged): radiobiology and dosimetry of alphaparticle emitters for targeted radionuclide therapy. J Nucl Med. 2010; 51:311-28. Available:https://doi.org/10.2967/jnumed.108.058651
4. Elgqvist J, Frost S, Pouget JP, Albertsson P. The potential and hurdles of targeted

alpha therapy–clinical trials and beyond. Frontiers in oncology. 2014;3 :324.
Available:https://doi.org/10.3389/fonc.2013.00324

5. Dziawer L, Koźmiński P, Męczyńska-Wielgosz S, Pruszyński M, Łyczko M, Wąs B, Celichowski G, Grobelny J, Jastrzebski J, Bilewicz A. Gold nanoparticle bioconjugates labelled with ^{211}At for targeted alpha therapy. RSC Adv. 2017;7:41024.
Available:https://doi.org/10.1039/C7RA06376H
6. Kaneda-Nakashima K, Zhang Z, Manabe Y, Shimoyama A, Kabayama K, Watabe T, Kanai Y, Ooe K, Toyoshima A, Shirakami Y, Yoshimura T. α-Emitting cancer therapy using 211At-AAMT targeting LAT1. Cancer science. 2021;112(3):1132-40.
Available:https://doi.org/10.1111/cas.14761
7. Ha H, Kwon H, Lim T, Jang J, Park SK, Byun Y. Inhibitors of prostate-specific membrane antigen in the diagnosis and therapy of metastatic prostate cancer–a review of patent literature. Expert Opinion on Therapeutic Patents. 2021;31(6):525-47.
Available:https://doi.org/10.1080/13543776.2021.1878145
8. Li HK, Morokoshi Y, Kodaira S, Kusumoto T, Minegishi K, Kanda H, Nagatsu K, Hasegawa S. Utility of 211At-trastuzumab for the treatment of metastatic gastric cancer in the liver: evaluation of a preclinical α-radioimmunotherapy approach in a clinically relevant mouse model. Journal of Nuclear Medicine. 2021;62(10):1468-74.
Available:https://doi.org/10.2967/jnumed.120.249300
9. Zalutsky MR, Pruszynski M. Astatine-211: Production and Availability. Curr. Radiopharm. 2011;4:177.
Available:https://doi.org/10.2174/1874471011104030177
10. Poty S, Francesconi LC, McDevitt MR, Morris MJ, Lewis JS. α-Emitters for radiotherapy: from basic radiochemistry to clinical studies—part 1. Journal of Nuclear Medicine. 2018;59(6):878-84.
Available:https://doi.org/10.2967/jnumed.116.186338
11. Huang D, Liao F, Molesa S, Redinger D, Subramanian V. Plastic-compatible low resistance printable gold nanoparticle conductors for flexible electronics. Journal of the electrochemical society. 2003; 150(7):G412.
Available:https://doi.org/10.1149/1.1582466
12. Haruta M, Kobayashi T, Sano H, Yamada N. Novel Gold Catalysts for the Oxidation of Carbon Monoxide at a Temperature far below 0°C. Chem. Lett. 1987;16:405.
Available:https://doi.org/10.1246/cl.1987.405
13. Yotsuhashi S, Yamada Y, Kishi T, Diño WA, Nakanishi H, Kasai H. Dissociative adsorption of O 2 on Pt and Au surfaces: Potential-energy surfaces and electronic states. Physical Review B. 2008;77(11):115413.
Available:https://doi.org/10.1103/PhysRevB.77.115413
14. Arevalo RL, Escaño MC, Kasai H. Mechanistic insight into the Au-3d metal alloy-catalyzed borohydride electro-oxidation: from electronic properties to thermodynamics. ACS Catalysis. 2013;3(12):3031-40.
Available:https://doi.org/10.1021/cs400735h
15. Arevalo RL, Aspera SM, Nakanishi H, Kasai H, Yamaguchi S, Asazawa K. Adsorption of Carbohydrazide on Au (111) and Au3Ni (111) Surfaces. Catalysis Letters. 2018;148(4):1073-9.
Available:Available:https://doi.org/10.1007/s10562-018-2327-2
16. Peng J, Liang X. Progress in research on gold nanoparticles in cancer management. Medicine. 2019;98:e15311.
Available:https://doi.org/10.1097/MD.0000000000015311
17. Li X, Zhang Y, Liu G, Zhou L, Xue Y, Liu M. Recent progress in the applications of gold-based nanoparticles towards tumor-targeted imaging and therapy. RSC advances. 2022;12(13):7635-51.
Available:https://doi.org/10.1039/D2RA00566B
18. Anik MI, Mahmud N, Al Masud A, Hasan M. Gold nanoparticles (GNPs) in biomedical and clinical applications: A review. Nano Select. 2022 Apr;3(4):792-828.
Available:https://doi.org/10.1002/nano.202100255
19. Yuan L, Zhang F, Qi X, Yang Y, Yan C, Jiang J, Deng J. Chiral polymer modified nanoparticles selectively induce autophagy of cancer cells for tumor ablation. Journal of nanobiotechnology. 2018;16(1):1-6.

Available:https://doi.org/10.1186/s12951-018-0383-9
20. Duncan B, Kim C, Rotello VM. Gold nanoparticle platforms as drug and biomacromolecule delivery systems. Journal of controlled release. 2010 Nov 20;148(1):122-7. Available:https://doi.org/10.1016/j.jconrel.2010.06.004
21. De Jong WH, Borm PJA. Drug delivery and nanoparticles: Applications and hazards. Int. J. Nanomedicine. 2008;3:133. Available:https://doi.org/10.2147/ijn.s596
22. Cai W, Gao T, Hong H, Sun J. Applications of gold nanoparticles in cancer nanotechnology. Nanotechnol. Sci. Appl. 2008;1:17. Available:https://doi.org/10.2147/NSA.S3788
23. Lopez-Marzo AM, Hoyos-de-la-Torre R, Baldrich E. NaNO3/NaCl Oxidant and Polyethylene Glycol (PEG) Capped Gold Nanoparticles (AuNPs) as a Novel Green Route for AuNPs Detection in Electrochemical Biosensors. Anal. Chem. 2018;90:4010. Available:https://doi.org/10.1021/acs.analchem.7b05150
24. Poty S, Francesconi LC, McDevitt MR, Morris MJ, Lewis JS. α-Emitters for Radiotherapy: From Basic Radiochemistry to Clinical Studies – Part 2. J. Nucl. Med. 2018;59:1020. Available:https://doi.org/10.2967/jnumed.117.204651
25. Walsh AA. Chemisorption of iodine-125 to gold nanoparticles allows for real time quantitation and potential use in nanomedicine. J. Nanopart. Res. 2017;19:152. Available:https://doi.org/10.1007/s11051-017-3840-8
26. Daems N, Michiels C, Lucas S, Baatout S, Aerts A. Gold nanoparticles meet medical radionuclides. Nuclear Medicine and Biology. 2021;100:61-90. Available:https://doi.org/10.1016/j.nucmedbio.2021.06.001
27. Kasai H, Akai H, Yoshida H. Computational Materials Design from Basics to Actual Applications (Osaka University Press, Suita, Japan; 2005. (in Japanese). ISBN: 978-4-87259-152-1
28. Kasai H, Tsuda M. Computational Materials Design, Case Study I: Intelligent/Directed Materials Design for Polymer Electrolyte Fuel Cells and Hydrogen Storage Applications (Osaka University Press, Suita, Japan; 2008) (in Japanese). ISBN: 978-4-87259-254-2
29. Kasai H, Escaño MCS. Eds. Physics of Surface, Interface, and Cluster Catalysis (IOP Publishing Bristol UK; 2016). Available:https://doi.org/10.1088/978-0-7503-1164-9
30. Kasai H, Padama AAB, Chantaramolee B, Arevalo RL. Hydrogen and Hydrogen-Containing Molecules on Metal Surfaces (Springer, Singapore; 2020). Available:https://doi.org/10.1007/978-981-15-6994-4
31. Aspera SM, Arevalo RL, Chantaramolee B, Nakanishi H, Kasai H. PdRuIr ternary alloy as an effective NO reduction catalyst: insights from first-principles calculations. Phys. Chem. Chem. Phys. 2021;23:7153-7163. Available:https://doi.org/10.1039/D0CP06453J
32. Kishida R, Aspera SM, Kasai H. Melanin Chemistry Explored by Quantum Mechanics (Springer, Singapore; 2021). Available:https://doi.org/10.1007/978-981-16-1315-9
33. Serov A, Aksenov N, Bozhikov G, Eichler R, Dressler R, Lebedev V, Petrushkin O, Piguet D, Shishkin S, Tereshatov E, Türler A, Vögele A, Wittwer D, Gäggeler HW. Adsorption interaction of astatine species with quartz and gold surfaces. Radiochim. Acta. 2011;99:593-599. Available:https://doi.org/10.1524/ract.2011.1850
34. Demidov Y, Zaitsevskii A. Adsorption of the astatine species on gold surface: A relativistic density functional theory study. Chem. Phys. Lett. 2018;691:126-130. Available:https://doi.org/10.1016/j.cplett.2017.11.008
35. Kresse G, Furthmüller J. Efficient iterative schemes for *ab initio* total-energy calculations using a plane-wave basis set. Phys. Rev. 1996;B 54:11169. Available:https://doi.org/10.1103/PhysRevB.54.11169
36. Kresse G, Furthmüller J. Efficiency of ab-initio total energy calculations for metals and semiconductors using a plane-wave basis set. Comput. Mater. Sci. B. 1996;6:15. Available:https://doi.org/10.1016/0927-0256(96)00008-0

37. Perdew JP, Burke K, Ernzerhof M. Generalized Gradient Approximation Made Simple. Phys. Rev. Lett. 1996;77:3865. Available:https://doi.org/10.1103/PhysRevLett.77.3865
38. Grimme S, Ehrlich S, Goerigk L. Effect of the Damping Function in Dispersed Corrected Density Functional Theory. J. Comput. Chem. 2011;32:1456. Available:https://doi.org/10.1002/jcc.21759
39. Blöchl PE. Projector augmented-wave method. Phys. Rev. B: Condens. Matter Mater. Phys. 1994;50:17953. Available:https://doi.org/10.1103/PhysRevB.50.17953
40. Kresse G, Joubert D. From ultrasoft pseudopotentials to projector augmented-wave method. Phys. Rev. B: Condens. Matter Mater. Phys. 1999;59:1758. Available:https://doi.org/10.1103/PhysRevB.59.1758
41. Monkhorst HJ, Pack JD. Special points for Brillouin-zone integrations. Phys. Rev. B: Condens. Matter Mater. Phys. 1976;13:12. Available:https://doi.org/10.1103/PhysRevB.13.5188
42. Lide DR, Ed. CRC Handbook of Chemistry and Physics (Taylor & Francis Group, Florida, 2005) 86th ed.:4-5. Available:https://doi.org/10.1021/ja059868l
43. Henkelman G, Arnaldson A, Jónsson H. A fast and robust algorithm for Bader decomposition of charge density. Comput. Mater. Sci. 2006;36:254. Available:https://doi.org/10.1016/j.commatsci.2005.04.010
44. Kleis J, Greeley J, Romero NA, Morozov VA, Falsig H, Larsen AH, Lu J, Mortensen JJ, Dulak M, Thygesen KS, Norskøv JK, Jacobsen KJ. Finite Size Effects in Chemical Bonding: From Small Clusters to Solids. Catal. Lett. 2011;141:1067. Available:https://doi.org/10.1007/s10562-011-0632-0
45. Grochola G, Snook IK, Russo SP. On the relative stabilities of gold nanoparticles. J. Chem. Phys. 2007;127:224704. Available:https://doi.org/10.1063/1.2789419
46. Holec D, Dumitraschkewitz P, Vollath D, Fischer FD. Surface Energies of Au Nanoparticles Depending on Their Size and Shape. Nanomaterials. 2020;10:484. Available:https://doi.org/10.3390/nano10030484

Peer-review history:
The peer review history for this paper can be accessed here:
https://www.sdiarticle5.com/review-history/93762